gel (0.1 g) followed by diazomethane in Et₂O[15] (2.6 M, 1 mL). After the solution was stirred for 1 h, silica gel (0.1 g) followed by diazomethane in Et₂O (2.6 M, 1 mL) was added. The mixture was maintained at 0 °C for 1 h and allowed to warm up to room temperature overnight. The silica gel was removed by filtration and washed with Et₂O (5 × 1 mL). The combined eluants were evaporated, and the residue was chromatographed on silica gel (eluant, 3:1 hexanes/EtOAc) to give **8a** (24 mg, 82%) as a colorless oil, which was identical by ¹H NMR and TLC with the major isomer reported above.

Preparation of Methyl (Methyl 2,3-*O*-isopropylidene-β-D-allofuranosid)uronate (9a) from Benzyl Ether 8b. To a solution of the benzyl ether **8b** (22 mg, 0.062 mmol) in MeOH (4 mL) was added palladium black (5 mg), and H₂ (ca. 1 L) was bubbled through the rapidly stirred mixture over 5 min. A static source of H₂ was attached and the mixture was allowed to stir for 48 h. The catalyst was removed by filtration through Celite, washed with MeOH (2 × 1 mL), and the solution evaporated. The residue was chromatographed on silica (eluant, 3:1 hexanes/EtOAc) to give **9a** (16 mg, 89%) as a colorless oil, which was identical by ¹H NMR and TLC with an authentic sample of **9a**.[5]

Preparation of Methyl (Methyl 2,3-*O*-isopropylidene-5-(toluene-4-sulfonamido)-5-deoxy-β-D-allofuranosid)uronate (8c) from Azide 9b. To a solution of the azide **9b**[5] (17 mg, 0.059 mmol) in MeOH (2 mL) was added palladium black (4 mg), and H₂ (ca. 1 L) was passed through the rapidly stirred mixture over 5 min. A static source of H₂ was attached

and the mixture was stirred for 30 min. The catalyst was removed by filtration through Celite, washed with MeOH (5 × 1 mL), and the solution evaporated. To the residue (16 mg) in CH₂Cl₂ (2 mL) at 0 °C was added *p*-TsCl (69 mg, 0.36 mmol), *iso*-Pr₂NEt (24 μL, 0.14 mmol), and DMAP (2 mg, 0.02 mmol). The reaction mixture was maintained at 0 °C for 4 h, poured into H₂O (10 mL), and extracted with Et₂O (3 × 10 mL). The combined organic layers were dried (MgSO₄) and evaporated. The residue was chromatographed on silica (eluant, 3:1 hexanes/EtOAc) to give **8c** (17 mg, 71%) as a white solid, which was identical by ¹H NMR and TLC with the major isomer reported above.

(15) Arndt, F. *Organic Syntheses*; Wiley: New York, 1943; Collect. Vol. II, 165.

Core Size and Flexibility of Metallohydroporphyrin Macrocycles. Implications for F₄₃₀ Coordination Chemistry

Warren A. Kaplan,[1a,b] **Kenneth S. Suslick,*,[1a]** **and Robert A. Scott*,[1c]**

Contribution from the School of Chemical Sciences, University of Illinois at Urbana—Champaign, Urbana, Illinois 61820, and the Departments of Chemistry and Biochemistry and the Center for Metalloenzyme Studies, University of Georgia, Athens, Georgia 30602. Received August 6, 1990

Abstract: We have used molecular mechanics calculations to investigate the effect of macrocycle reduction on core-hole size and flexibility of a series of metallo(hydro)porphyrin molecules. Macrocycle reduction at β-pyrrole positions results in an increase in core size, whereas reduction at methine positions results in a decrease in core size. The tetrapyrroles are found to become significantly more flexible (susceptibile to S₄ ruffling) only when reduction occurs at methine positions. These results are used to explain the unique ligand-binding ability of the nickel–tetrapyrrole F₄₃₀ cofactor of the *S*-methyl coenzyme M reductase enzyme of methanogenic bacteria. Molecular mechanics also predicts the increased axial-ligand affinity of the native F₄₃₀ isomer compared to the 12,13-diepimer, as a result of the increase in macrocycle torsional strain in the 4-coordinate native isomer.

The final step of archaebacterial methanogenesis (eq 1) involves F₄₃₀, the nickel-containing cofactor of *S*-methyl coenzyme M

$$CH_3SCoM + HSHTP \rightarrow CH_4 + CoMSSHTP \qquad (1)$$
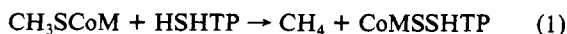
reductase.[2,3] F₄₃₀ possesses the most highly reduced 16-membered tetrapyrrolic macrocycle yet encountered in nature (Figure 1). The precise role of F₄₃₀ in methane production remains unknown, but could involve redox, substrate binding (i.e., coenzyme M or

N-7-mercaptoheptanoyl-*O*-phospho-L-threonine, HSHTP), or methyl transfer. Investigation of the chemical reactivity of F₄₃₀ will help evaluate this role.

The Ni(II) ion of F₄₃₀ is the most electrophilic metal center of a series of nickel-containing hydroporphyrin complexes.[4] Three factors have been proposed to contribute to the unique ligand-binding ability of F₄₃₀.

(a) Steric Inhibition of S₄ Ruffling. This ruffling is known to occur in nickel-containing hydroporphyrins[5-9] and reduces the

(1) (a) University of Illinois. (b) Present address: Dow Chemical, Urethane Chemicals Research, Texas Operations, B-1470, Freeport, TX 77541. (c) University of Georgia.

(2) Abbreviations used: CH₃SCoM, *S*-methyl coenzyme M (2-(methylthio)ethanesulfonic acid); HSHTP, *N*-7-mercaptoheptanoyl-*O*-phospho-L-threonine; hexahydroporphyrin, 1,2,3,7,8,20-hexahydroporphyrin; pyrrocorphin, 2,3,7,8,12,13-hexahydroporphyrin; isobacteriochlorin, 2,3,7,8-tetrahydroporphyrin; chlorin, 2,3-dihydroporphyrin; metallo(hydro)porphyrin refers generally to metal complexes of porphyrins or hydroporphyrins.

(3) Wolfe, R. S. *Trends Biochem. Sci.* **1985**, *10*, 396–399.

(4) Kratky, C.; Fässler, A.; Pfaltz, A.; Kräutler, B.; Jaun, B.; Eschenmoser, A. *J. Chem. Soc., Chem. Commun.* **1984**, 1368–1371.

(5) Suh, M. P.; Swepston, P. N.; Ibers, J. A. *J. Am. Chem. Soc.* **1984**, *106*, 5164–5171.

(6) Kratky, C.; Waditschatka, R.; Angst, C.; Johansen, J. E.; Plaquevent, J. C.; Schreiber, J.; Eschenmoser, A. *Helv. Chim. Acta* **1985**, *68*, 1312–1337.

(7) Waditschatka, R.; Kratky, C.; Jaun, B.; Heinzer, J.; Eschenmoser, A. *J. Chem. Soc., Chem. Commun.* **1985**, 1604–1607.

(8) Stolzenberg, A. M.; Stershic, M. T. *Inorg. Chem.* **1987**, *26*, 1970–1977.

Native F$_{430}$　　　　　　　12,13-diepimer
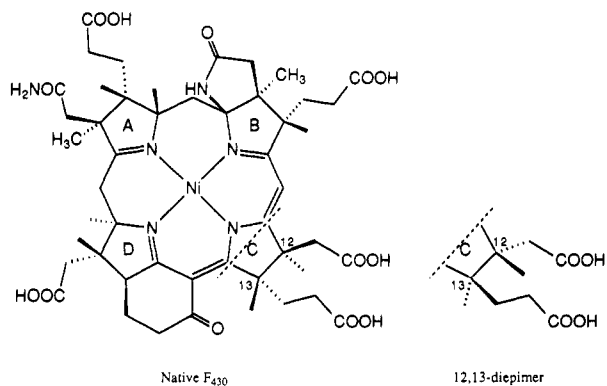
Figure 1. Spectroscopically derived structures of F$_{430}$ and its 12,13-di-epimer.

macrocycle core size. In F$_{430}$, inhibition of ruffling would de-stabilize the 4-coordinate, low-spin state.

(b) Core-Hole Expansion. Tetrapyrrole reduction often results in larger cavity sizes, decreasing the ligand field strength of the macrocycle, thus increasing axial ligand affinity.

(c) Increase in Macrocycle Flexibility. Tetrapyrrole reduction has often been proposed to result in greater macrocycle flexibility.[5,9-11] Enhanced flexibility would allow for macrocycle adjustment to reduce any steric interactions between the axial ligand and the macrocycle core and would accommodate the increase in Ni(II) ionic size that accompanies the increase in coordination number.[12]

To investigate the contribution of these factors to the ligand-binding properties of F$_{430}$, we have undertaken molecular mechanics[13] calculations. It has been proposed that the F$_{430}$ macrocycle is flexible enough to adopt a trigonal-bipyramidal 5-coordinate geometry (with one additional ligand).[14] However, our calculations confirm the finding[14] that the square-planar form is lower in energy than the nonpolanar conformation appropriate for the hypothetical monoligated trigonal-bipyramidal form.[15] It should be emphasized that our calculations put no constraints on the Ni geometry (vide infra). We have therefore chosen to examine the effect of tetrapyrrole reduction on binding of axial ligands and on its flexibility toward "in-plane" (S$_4$-type) deformations. The results presented here suggest that both factors (a) and (c) are important in determining the ligand-binding properties of F$_{430}$.

Computational Methods

Molecular mechanics calculations utilized version 1.5 of the Biograf software package (Biodesign, Inc.; Pasadena, CA) using the MMP2 force field.[16,17] The following parameters have been used instead of, or in addition to, the standard MMP2 parameters: porphyrin C$_{sp^2}$–C$_{sp^2}$ bond stretch force constant = 1381 kcal·mol^{-1}·Å^{-2}, equilibrium distance = 1.390 Å; porphyrin N$_{sp^2}$–C$_{sp^2}$ bond strength force constant = 906 kcal·mol^{-1}·Å^2, equilibrium distance = 1.350 Å; N$_{sp^2}$–C$_{sp^3}$ bond stretch force constant = 506 kcal·mol^{-1}·Å^{-2}, equilibrium distance = 1.470 Å; imidazole N$_{sp^2}$–C$_{sp^2}$–C$_{sp^2}$–C$_{sp^3}$ torsional barrier = 10.0 kcal·mol^{-1}, minimum torsion angle = 180°; imidazole C$_{sp^2}$–N$_{sp^2}$–C$_{sp^2}$–C$_{sp^3}$ torsional barrier = 10.0
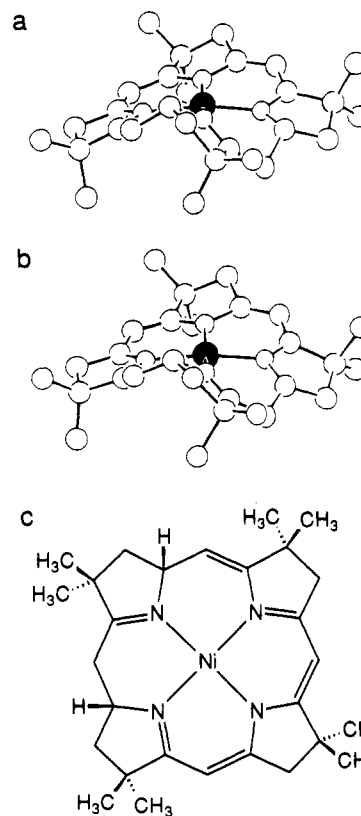
Figure 2. Comparison of the molecular mechanics energy minimized structure (a) and the X-ray crystal structure (b) for (2,2,7,7,12,12,17,17-octamethyl-2,3,4,7,8,12,13,18,19,20-decahydro-17H-porphinato)nickel(II) (c). The combined rms difference in atomic position for 25 matched core atoms was 0.13 Å. The molecular mechanics derived (crystal structure) values for some important parameters are the following: average Ni–N distance, 1.908 (1.899) Å; average N–Ni–N angle, 168.3° (168.4°); *trans* pyrrole dihedral angle, 32.6° (33.5°).

kcal·mol^{-1}, minimum torsion angle = 180°.

For calculations involving comparison of the isomers of F$_{430}$, the following parameters have been used to define the high-spin nickel(II) ion: Ni–N bond stretch force constant = 288 kcal·mol^{-1}·Å^{-2}, equilibrium distance = 2.09 Å; Ni nonbond radius = 5.0 Å, well depth = 0.17 kcal·mol^{-1}. The following parameters have been used to define the low-spin nickel(II) ion: Ni–N bond stretch force constant = 288 kcal·mol^{-1}·Å^{-2}, equilibrium bond distance = 1.86 Å; Ni nonbond radius = 4.8 Å, well depth = 0.17 kcal·mol^{-1}.

To allow the nickel ion to adopt coordination geometries other than the strict square-planar or octahedral forms, no force constant constraints were placed on the N–Ni–N bond angles or the C–C–N–Ni torsion angles of the metallohydroporphyrin. This allows the F$_{430}$ isomers to (computationally) adopt the conformations forced upon them by the steric interactions of the hydroporphryin and its substituents, as well as any added imidazole ligands. In the calculations involving the 6-coordinate F$_{430}$ forms, the structures were minimized with the inclusion of all axial ligand interactions with the hydroporphyrin. To allow direct comparison of the energies of the 4- and 6-coordinate species, the *minimized* steric energies of the 6-coordinate forms have been expressed without the contribution of the axial ligands. In this way we could evaluate the relative strains placed upon the hydroporphyrin complexes by axial ligation.

The core-size energy comparisons were performed by varying the equilibrium Ni–N bond distance while keeping unchanged the bond-stretch force constant at 288 kcal·mol^{-1}·Å^{-2} for each chosen bond length. The metal ion was given a nonbonded van der Waals radius of zero for these calculations to remove the (hypothetical) metal ion from calculated atom-atom repulsions. This allows the relative core size of the hydroporphyrin to be determined without regard to the nature of the metal ion being coordinated. For very long M–N bond distances, there was a tendency for the metal to minimize out of the plane of the macrocycle. To produce a local minimum in which the metal remained within the macrocycle plane, minimizations were performed with large N–M–N angle bend force constants (100 kcal·mol^{-1}·deg^{-2}, equilibrium angle =

(9) Fajer, J.; Barkigia, K. M.; Goff, D. A. In *Porphyrins. Excited States and Dynamics*; Gouterman, M., Rentzepis, P. M., Straub, K. D., Eds.; American Chemical Society: Washington, DC, 1986; ACS Symp. Ser. 321, pp 51–58.

(10) McRee, D. E.; Richardson, D. C.; Richardson, J. S.; Siegel, L. M. *J. Biol. Chem.* **1986**, *261*, 10277–10281.

(11) Scheidt, W. R.; Lee, Y. J. *Struct. Bonding* **1987**, *64*, 1–70.

(12) Thöm, V. J.; Hancock, R. D. *J. Chem. Soc., Dalton Trans.* **1985**, 1877–1880.

(13) Burkert, U.; Allinger, N. L. *Molecular Mechanics*; American Chemical Society: Washington, DC, 1982.

(14) Zimmer, M.; Crabtree, R. H. *J. Am. Chem. Soc.* **1990**, *112*, 1062–1066.

(15) Kaplan, W. A., Ph.D. Thesis, University of Illinois at Urbana—Champaign, 1990.

(16) Allinger, N. L.; Flanagan, H. L. *J. Comp. Chem.* **1983**, *4*, 399–403.

(17) Liljefors, T.; Tai, J. C.; Li, S.; Allinger, N. L. *J. Comp. Chem.* **1987**, *8*, 1051–1056.

F₄₃₀   Hexahydroporphyrin

Pyrrocorphin   Isobacteriochlorin

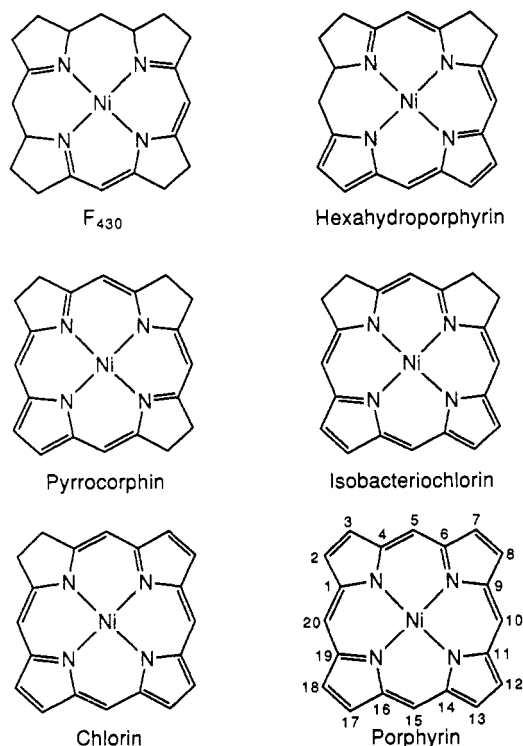Chlorin   Porphyrin

Figure 3. Core structures of the Ni(II) (hydro)porphyrins investigated.

180°). Minimized energies were then determined without the contribution of these angular terms. No (hydro)porphyrin substituents have been included in these calculations so that the effect of core size due solely to the macrocycle's reduction level could be determined.[18]

All molecules examined in this study have been subjected to extensive molecular dynamics calculations and reminimized multiple times to ensure attainment of global minima. The dynamics calculations were performed using the molecular dynamics subroutine within Biograf (Straight Dynamics). In general, molecular dynamics were run for 2.0 ps in vacuo at 300 K using 0.002-ps time steps. After reminimization, if a structure of lower energy was found, the dynamics and minimization process was repeated.

The reliability of the MMP2 force field was established by the ability of molecular mechanics to reproduce experimentally observed structures for a series of metallohydroporphyrins.[15,19,20] Comparison of the crystal structure[21] of (2,2,7,7,12,12,17,17-octamethyl-2,3,4,7,8,12,13,18,19,20-decahydro-17*H*-porphinato)nickel(II) with the energy-minimized structure (Figure 2) gives an indication of the "geometric reliability" of the force field for a highly reduced tetrapyrrole whose electronic structure is similar to that of F₄₃₀.

Results and Discussion

We have addressed two aspects of F₄₃₀ Ni(II) ligation using molecular mechanics. First, the experimentally determined difference in ligand-binding affinity of the native and 12,13-diepimeric conformations of F₄₃₀ has been rationalized. Native F₄₃₀ has *at least* a 40-fold greater affinity for imidazole ligands than does the diepimer; the difference in the experimental free energies of imidazole binding is >2.6 kcal·mol⁻¹ in ethanol at 298 K.[22] Considering only macrocycle energetics, molecular mechanics calculations predict the steric energy costs of ligand binding to be 3.0 kcal·mol⁻¹ less for F₄₃₀ than for the diepimer.[23] The

Table I. Molecular Mechanics Derived Cavity Sizes and Relative Macrocycle Flexibilities for Selected (Hydro)porphyrins

macrocycle[a]	cavity size ideal M–N distance,[b] Å	rel flexibility,[c] kcal·mol⁻¹·Å⁻²
porphyrin	2.03	506
chlorin	2.05	489
isobacteriochlorin	2.07	481
pyrrocorphin	2.09	463
hexahydroporphyrin	2.05	284
F₄₃₀	2.00	156

[a] See Figure 3 for core structures. [b] M–N distance at minimum in molecular mechanics derived energy. [c] Coefficient α in a fit of energy (E) vs M–N distance (d) to $E = \alpha d^2 + \beta d + \gamma$.
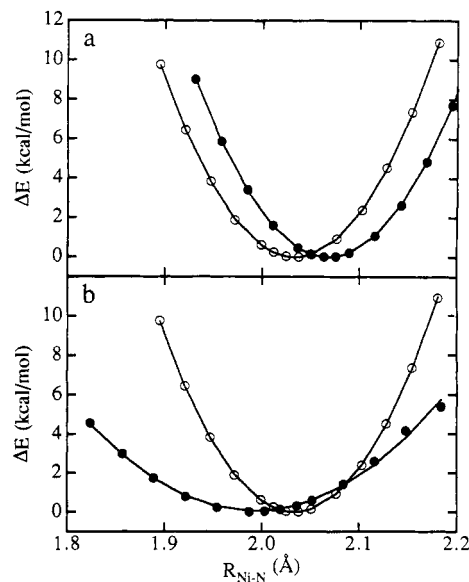

Figure 4. Comparison of molecular mechanics derived energies of selected (hydro)porphyrins as a function of M–N distance: (a) porphyrin (O) compared to isobacteriochlorin (●); (b) porphyrin (O) compared to F₄₃₀ (●). The solid lines are second-order polynomial fits, the quadratic coefficients of which appear in Table I.

calculations suggest that 4-coordinate F₄₃₀ binds axial ligands with higher affinity than 4-coordinate diepimer because of specific torsional strains that prevent 4-coordinate F₄₃₀ from ruffling easily.[23,24]

We have also used molecular mechanics to assess the basis of the increased ligation affinity of F₄₃₀ over other Ni(II) (hydro)porphyrins. Calculations have been used to determine the core size of (hydro)porphyrins as a function of macrocycle reduction. The variability in the core size of the macrocycle influences the ligand-binding ability of the resulting metallo(hydro)porphyrin complex. This relationship between electrophilicity at the metal center and the macrocycle core-hole size is a general phenomenon and has been documented in other (non-tetrapyrrole) systems.[25] Molecular mechanics has been used to determine the core size for a variety of tetraaza and pentaaza macrocycles,[25-29]

(18) It should be noted that the inclusion of ethyl substituents at the β-pyrrole positions of the macrocycle does not have an effect on the relative core sizes and flexibilities determined.

(19) Kaplan, W. A.; Scott, R. A.; Suslick, K. S., manuscript in preparation.

(20) For ten minimized structures (two Ni(II) porphyrins, two Ni(II) chlorins, two Ni(II) (iso)bacteriochlorins, three Ni(II) hexahydroporphyrins, and one Ni(II) decahydroporphyrin), the average rms deviation of calculated vs observed atomic positions for 25 matched core atoms was 0.12 Å.[15]

(21) Fässler, A.; Pfaltz, A.; Müller, P. M.; Farooq, S.; Kratky, C.; Kräutler, B.; Eschenmoser, A. *Helv. Chim. Acta* **1982**, *65*, 812–827.

(22) Shiemke, A. K.; Kaplan, W. A.; Hamilton, C. L.; Shelnutt, J. A.; Scott, R. A. *J. Biol. Chem.* **1989**, *264*, 7276–7284.

(23) Detailed molecular mechanics energies (kcal·mol⁻¹) are as follows: 4-coordinate native, 74.6 (bond stretch, 6.9; angle bend, 31.5; torsion, 28.7; van der Waals, 7.6); 6-coordinate native, 76.7 (bond stretch, 5.5; angle bend, 34.7; torsion, 24.1; van der Waals, 12.5); 4-coordinate diepimer, 73.1 (bond stretch, 5.0; angle bend, 33.5; torsion, 26.0; van der Waals, 8.6); 6-coordinate diepimer, 78.3 (bond stretch, 4.4; angle bend, 35.8; torsion, 25.8; van der Waals, 12.3).

(24) Other possible factors contributing to the enhanced ligand affinity of native F₄₃₀ over the diepimer include differential metal–ligand bond strengths and differential solvation effects. We believe these are minor factors, based on the identical spectroscopic characteristics of ligand-bound native and diepimeric derivatives.[22]

(25) Busch, D. *Acc. Chem. Res.* **1978**, *11*, 392–400.

(26) Drew, M. G. B.; Rice, D. A.; Silong, S. B.; Yates, P. C. *J. Chem. Soc., Dalton Trans.* **1986**, 1081–1086.

(27) Drew, M. G. B.; Hollis, S.; Yates, P. C. *J. Chem. Soc., Dalton Trans.* **1985**, 1829–1834.

and we have used a similar procedure to evaluate core sizes of a number of metallo(hydro)porphyrins. Core structures for the Ni(II) (hydro)porphyrins examined are in Figure 3. The minimum in a plot of total energy (including all bond stretch, bond angle bend, torsion, and van der Waals interactions) versus optimized M–N bond distance represents the ideal core size for a given tetrapyrrole. The chosen M–N stretch force constant does not affect the position of this minimum, but it *does* affect the steepness of the potential curve generated. This steepness (which is objectively quantified by fitting the curve to a second-order polynomial and extracting the quadratic coefficient) can be considered a measure of the flexibility of the macrocycle toward ruffling distortions. If the same M–N stretch force constant is used for each of the macrocycles studied,[30] a relative measure of the macrocycle flexibilities is obtained.

The core radii and relative macrocycle flexibility for the porphyrin, chlorin, isobacteriochlorin, pyrrocorphin, hexahydroporphyrin, and F_{430} macrocycles (Figure 3) are summarized in Table I. Molecular mechanics results indicate that macrocycle core size *increases* when reduction occurs at β-pyrrole positions (cf., porphyrin, chlorin, isobacteriochlorin, pyrrocorphin). In contrast, the core size apparently *decreases* when reduction occurs at methine positions (cf., hexahydroporphyrin, F_{430}). In addition, macrocycle flexibility *does not* increase significantly when a metalloporphyrin is reduced at β-pyrrole positions (Table I and Figure 4a). This is in excellent agreement with the experimental determination that metalloisobacteriochlorins are no more flexible than metalloporphyrins.[31] The calculations predict that reduction at methine positions, however, *does* increase the flexibility of the

macrocycle. The F_{430} macrocycle, a tetrapyrrole reduced at two adjacent methine positions (Figure 3), is the most flexible macrocycle examined. The predicted flexibility differences between porphyrin and F_{430} are dramatically apparent in Figure 4b.

Conclusions

The molecular mechanics calculations rationalize the relatively high affinity of F_{430} for axial ligands. It is reduction at the two methine carbons that provides the F_{430} macrocycle with the flexibility necessary to accommodate both high-spin (6-coordinate) and low-spin (4-coordinate, square-planar) Ni(II). This flexibility is expected to be important in a hypothetical substrate-binding role for F_{430} Ni(II). Since Ni(I) displays a larger ionic radius than low-spin Ni(II), a physiological redox role for F_{430} would also benefit from such flexibility.[32] In addition, molecular mechanics calculations show that relief of torsional strains caused by peripheral substituents is responsible for the greater stability (and decreased ligand-binding affinity) of the 4-coordinate ruffled form of the 12,13-diepimer of F_{430} compared to that of the native cofactor. Finally, the F_{430} macrocycle does not exhibit a larger core hole compared to more oxidized (hydro)porphyrins. Thus, macrocycle core-hole expansion *does not* contribute to the increased affinity of F_{430} for axial ligands.

(28) Thöm, V. J.; Fox, C. C.; Boeyens, J. C. A.; Hancock, R. D. *J. Am. Chem. Soc.* **1984**, *106*, 5947–5955.

(29) Hancock, R. D. *J. Chem. Soc., Dalton Trans.* **1986**, 2505–2506.

(30) As discussed in Computational Methods, the core size comparisons were made by varying the equilibrium bond distance while keeping the bond-stretch force constant at 288 kcal·mol⁻¹·Å⁻² for each chosen bond length. The metal ion was given zero size for these calculations by using a nonbond radius of zero for the metal.

(31) Kaplan, W. A.; Scott, R. A.; Suslick, K. S. *J. Am. Chem. Soc.* **1990**, *112*, 1283–1285.

(32) Furenlid, L. R.; Renner, M. W.; Fajer, J. *J. Am. Chem. Soc.* **1990**, *112*, 8987–8989.